

Thermal Structure of the Equatorial Topside Ionosphere*

B. C. NARASINGA RAO & RISAL SINGH

Radio Science Division, National Physical Laboratory, New Delhi 12

Manuscript received 3 April 1972

The thermal structure of the equatorial topside ionosphere is theoretically investigated to explain the experimentally observed features, viz. (i) isothermal region in the 400-500 km range, (ii) close coupling of electron and ion temperatures, and (iii) lower temperatures compared to mid-latitudes. The main reasons for these features seem to be the larger electron densities in the 400-500 km range and the absence of protonospheric heat flux flowing into the topside ionosphere. The theoretical profiles, calculated on the above basis, are found to be in good agreement with the experimentally observed profiles in the 400-1000 km region.

Introduction

THE experimental observations on the day-time electron and ion temperature (T_e , T_i) distributions in the topside ionosphere show different features in the equatorial and mid-latitudes. The equatorial profiles are available from the Thomson back-scatter radar observations made at Jicamarca¹⁻³ and the mid-latitude profiles are available from similar observations over Arecibo⁴, St Santin⁵ and Millstone Hill⁶ and from rocket observations over Wallops Island⁷. The major differences observed in the variation of T_i and T_e in the topside ionosphere between 400 and 1000 km region for low solar activity conditions are as follows:

1. At 400 km altitude over the equator the T_e and T_i are very close to the neutral temperature (T_n), which is about 900 K, whereas at mid-latitudes T_e is greater, being about 2000 K and T_i is near to 1000 K.
2. The height variation of T_e over the equator shows an isothermal region up to about 500 km and then T_e rises with height and reaches about 2000 K at 1000 km, whereas at mid-latitudes T_e is continuously rising above 400 km and reaches about 3000 K at 1000 km.
3. The T_i values in the entire height range 400-1000 km are almost same as T_e at equator, whereas at mid-latitudes T_i is nearer to T_n at 400 km and increases with height and becomes closer to T_e at 1000 km.

In this study, we have attempted to find out the causes responsible for these differences and then estimated theoretically the temperature profiles and compared them with the experimental observations.

Theory and Method of Investigation

The temperature distribution in the topside ionosphere is determined by heat input due to photoelectron heating, heat loss due to collisions with ions and neutrals, and heat loss due to conduction. The steady state energy balance equation for electrons

*Paper presented to the Physics Section of the 59th Session of the Indian Science Congress, held at Calcutta in February 1972.

may be written as

$$-\frac{d}{ds} \left(K_e \frac{dT_e}{ds} \right) = Q - L_e \quad \dots(1)$$

where K_e is the thermal conductivity of electrons given by $7.7 \times 10^6 T_e^{5/2}$ eV cm⁻¹ sec⁻¹ deg⁻¹, Q is the rate of heat input to electrons, L_e is the rate of heat loss of electrons and s is the distance along the geomagnetic field line.

We find that the heat input as calculated from the observed photoelectron fluxes and ambient electron densities is not very different between the equator and mid-latitudes, to a first approximation. These values are similar to those given by Nagy *et al.*⁸. The heat loss rates will, however, be very different for two reasons. Firstly, the electron densities, which control the collisional loss rate, are larger in the equatorial region compared to mid-latitudes. Secondly, the protonospheric heat flux, which has great influence on the temperature distribution in the mid-latitudes (Evans and Mantas⁹, Rao¹⁰) is absent in the equatorial region since the geomagnetic field lines do not extend beyond about 1000 km. These two factors are taken into account in theoretically estimating the temperature profiles in the equatorial region. It may be pointed out that it is essential to solve the above equation [Eq. (1)] along the geomagnetic field line, since in the equatorial region the geomagnetic field line curvature is more in the altitudes of our interest.

The collisional heat loss occurs due to collisions with various neutral particles (L_{en}) and ions (L_{ei}). At heights above 400 km, L_{ei} predominates over L_{en} . The ion temperature may be obtained by equating heat gained by ions from collisions with the electrons (L_{ei}) to the heat lost by collisions with the neutrals (L_{in}), since the thermal conduction of ions is relatively small. The functional forms and the coefficients are taken from Banks¹¹ and were given in our earlier work (Rao¹⁰).

The procedure adopted to solve the heat conduction equation is somewhat similar to the one employed by Evans and Mantas⁹ and is a slightly modified version of the one used earlier (Rao¹⁰). As in our earlier work, this equation is solved numerically by the Runge-Kutta method. As the equation

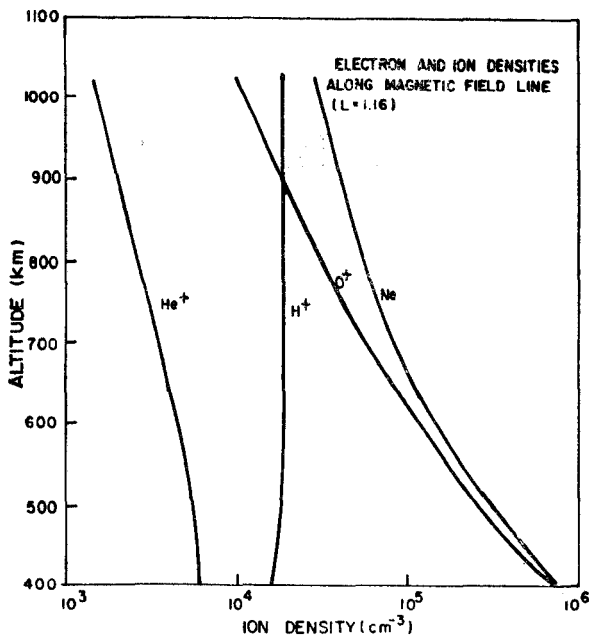


Fig. 1 — Electron and ion densities along the geomagnetic field line, $L=1.16$, as deduced from the latitudinal variations of average day-time electron densities for December solstice 1962-63, with Alouette-I [Ion composition information from Jicamarca and Arecibo are also utilized]

is a second order differential equation, it needs two boundary conditions to get the exact solution. The upper boundary condition is that the heat flux flowing down the field line at the equator, i.e. at the apex of the field line, is zero. The lower boundary condition may be set by choosing the proper value of T_e as determined by local heat balance between Q and L_{ei} since the conduction flux at this height is negligible as the experimentally observed temperature gradient is small (McClure²). For calculating the loss terms we need both ion and neutral densities. The neutral densities are taken from Jacchia¹² model atmosphere corresponding to exospheric temperature of 900 K which represents the day-time minimum solar activity condition. The ion densities along the geomagnetic field lines have to be constructed from various measurements. Some ionospheric composition profile data are available over Jicamarca¹ (1° mag. lat.) and Arecibo¹³ (30° mag. lat.). Using these data we have interpolated the percentages of O⁺, He⁺ and H⁺ ion densities to get them over the intermediate latitudes. Further, the average electron density contours observed with Alouette-I over the equator (Chan and Colin¹⁴) are used to obtain the electron density profiles along different magnetic field lines in the equatorial region. Combining them with the composition percentage data, we can get the ion density profiles along the geomagnetic field lines. One such profile obtained along the field line, $L = 1.16$, which starts at 400 km at 17° mag. lat. and reaches 1020 km over the equator, is shown in Fig. 1. Similarly the ion density profiles are constructed for various field lines decreasing in L value from 1.16 to 1.08 which reach the altitudes of 1020 km to 510 km over the equator. These ion densities are then used to solve the heat conduction equation.

Results and Discussion

The T_e and T_i variations along the different equatorial field lines are calculated by the method

described in the earlier section. In Fig. 2, the calculated temperature profiles for $L = 1.16$ are shown and compared with mid-latitude profiles as given in our earlier work (Rao¹⁰), for $L = 1.5$ (30° mag. lat.). The equatorial profile shows that (i) there is very close coupling between T_e and T_i throughout the altitude range, (ii) at 400 km they are almost same as T_n , and (iii) at 1000 km (over the equator) they reach a value of about 1800 K. Compared to the above features the mid-latitude temperature profiles are very different, being larger both

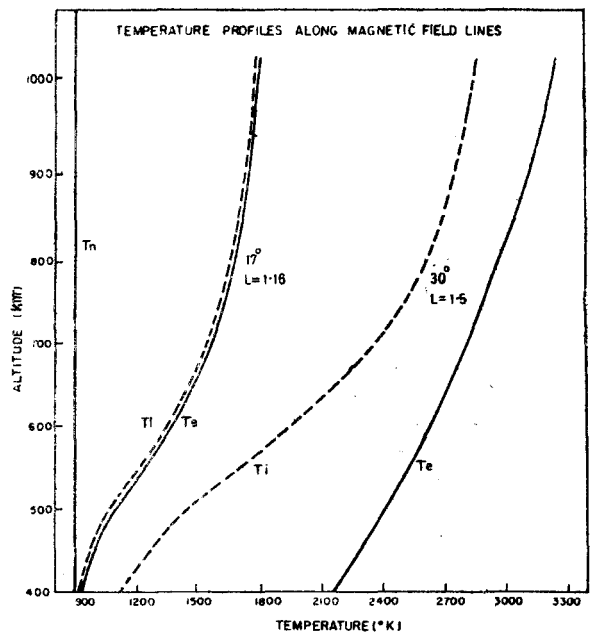


Fig. 2 — Comparison of the theoretical T_e and T_i profiles for equatorial and mid-latitude regions [The protonospheric heat flux flowing into the topside ionosphere at 1000 km is taken to be zero for equatorial profile and 4×10^9 eV cm⁻² sec⁻¹ for mid-latitude profile]

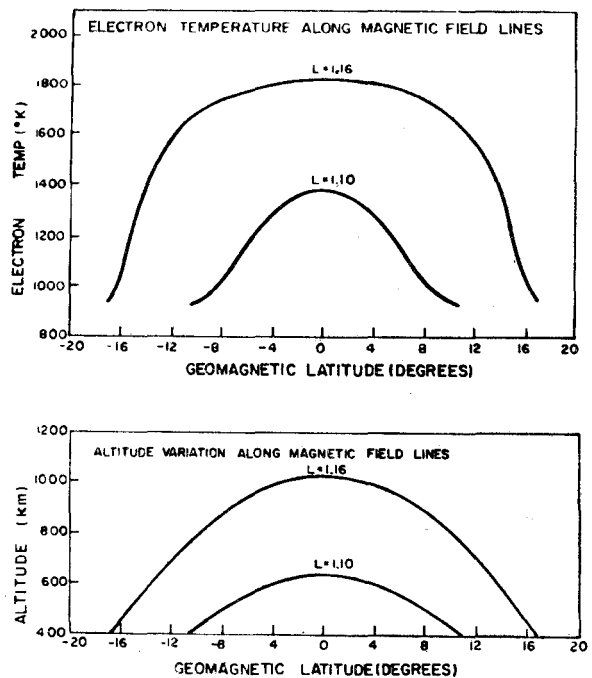


Fig. 3 — Theoretical T_e profiles along the two equatorial field lines, $L=1.16$ and $L=1.1$ [The height variations along these field lines are also shown (lower figure)]

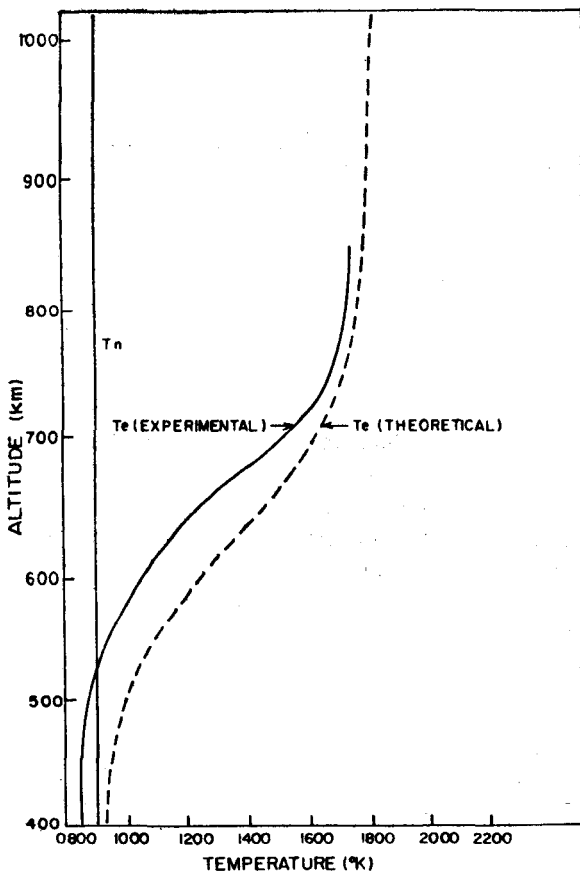


Fig. 4—Comparison of the theoretically evaluated height distribution of T_e over the equator with the experimentally observed distribution over Jicamarca on 2nd April 1966 at 1147 LT

at 400 and 1000 km altitudes with varying differences between T_e and T_i values.

To get a vertical profile of temperature over the equator we have calculated temperatures along different field lines over the equator. In Fig. 3, we have shown examples along two field lines, $L = 1.16$ and $L = 1.1$. Since T_i is very close to T_e in this region, T_i variation is not shown separately. The altitude variations of these field lines are also shown in the same figure. From such profiles the vertical

T_e profile is drawn and is shown in Fig. 4. For comparison one of the observed midday profiles over Jicamarca¹ is also shown. The theoretical profile shows all the features of the experimentally observed profile. The altitude variation is very little in the 400-500 km range and also in the 750-1000 km range, and large in between 500 and 750 km both in the theoretical and observed profiles. The lower value of 850 K at 400 km in the observed profile indicates that the neutral temperature is lower than that value at the time of observation. It is possible to get closer agreement by using a model atmosphere with exospheric temperature of 850 or 800 K.

The agreement between the theoretical and experimental profiles indicates that the two basic causes listed in the previous section are mainly responsible for the special type of thermal behaviour in the equatorial topside ionosphere.

Acknowledgement

The authors are thankful to Shri V. C. Jain for his help in computer programming. One of them (R.S.) is thankful to the CSIR, New Delhi, for the award of a junior research fellowship during the course of this work.

References

1. FARLEY, D. T., McCLURE, J. P., STERLING, D. L. & GREEN, J. L., *J. geophys. Res.*, **72** (1967), 5837.
2. McCLURE, J. P., *J. geophys. Res.*, **74** (1969), 279.
3. McCLURE, J. P., *J. geophys. Res.*, **76** (1971), 3106.
4. MAHAJAN, K. K., *J. atmos. terr. Phys.*, **29** (1967), 1137.
5. CARRU, H., PETIT, M. & WALDTEUFEL, P., *J. atmos. terr. Phys.*, **29** (1967), 351.
6. EVANS, J. V., *Planet. Space Sci.*, **15** (1967), 1557.
7. BRACE, L. H., MAYR, H. G. & FINDLAY, J. A., *J. geophys. Res.*, **74** (1969), 2952.
8. NAGY, A. F., FONTHEIM, E. G., STOLARSKI, R. S. & BEUTLER, A. E., *J. geophys. Res.*, **74** (1969), 4667.
9. EVANS, J. V. & MANTAS, G. P., *J. atmos. terr. Phys.*, **30** (1968), 563.
10. RAO, B. C. N., *Indian J. pure appl. Phys.*, **9** (1971), 501.
11. BANKS, P. M., *J. geophys. Res.*, **72** (1967), 3365.
12. JACCHIA, L. G., *Smithsonian Astrophysical Observatory Special Report 332*, 1971.
13. CARLSON, H. C. & GORDON, W. E., *J. geophys. Res.*, **71** (1966), 5573.
14. CHAN, K. L. & COLIN, LAWRENCE, *Proc. IEEE*, **57** (1969), 990.